

Inertia Effects on Virtual Contact Dynamics in Haptic Displays

L.L. Kovács* and **J. Kövecses**

Centre for Intelligent Machines,
Mechanical Engineering, McGill University
817 Sherbrooke Street West, H3A 0C3 Montreal, Canada
laszlokovacs@gmail.com, jozsef.kovecses@mcgill.ca

Abstract

Haptic systems provide force feedback to the human operator that enables the kinesthetic and/or tactile sensation of virtual environments. In case of kinesthetic devices, the human operator physically interacts with the haptic device at its reference element and the virtual environment forces are implemented at the actuators of the device. Compared to physical contacts, a major difference here is that the virtual contact is developed through internal reaction forces. The nature of these forces depends on the applied control strategy and the overall mechanical properties of the system.

Kinesthetic haptic devices are essentially robotic manipulators with low inertia and back-drivable transmission systems. These features help the transparent operation outside of the virtual environment, i.e., the device does not restrict much the free motion of the operator. The low inertial properties, structural flexibility, and the digital realization of the rendering algorithms may, however, lead to unstable operation of the haptic device. A large body of the literature focus on maintaining system stability and increasing the impedance range of the device. For the analysis of the dynamics, the majority of past work consider only single degree-of-freedom models. More detailed mass-spring-damper type models are reported in [1], but still the developed models are restricted to one specific axis of the investigated haptic devices. The parameters of these models are typically identified based on the frequency response of the system.

The human operator is typically considered in the form of impedance elements acting in direction of motion of the simplified mechanical model. A list of experimentally identified parameters are reported and used for stability analysis in [2]. The reported values span a wide range. For example, the mass of human operator is ranging from 0.15 to 17.51 kg. Clearly, these must correspond to very different experimental conditions and this difference in the inertia parameters can only be explained by considering the posture dependent nature of the effective mass of the human arm.

The concept of effective inertia parameters is described in detail in [3] for serial manipulators with different sub-chains. The provided results are directly applicable to haptics when soft grasp is considered, and the human-device interconnection may be modelled by a generalized spring and damper. For rigid grasps, the human and the haptic device forms a closed-chain which combined effective mass is essentially different than that of the device and the human arm separately. In the present paper we outline how the combined effective mass, affects the the impedance range that the device can render to the user. A novel formulation for the calculation of the effective mass is briefly summarized and verified by simulation with realistic parameters.

The effective mass play an important role in characterizing the virtual contact dynamics. Based on that, the mass/inertia parameters of different single degree-of-freedom models used in the literature can be identified all at once in a parametric form. According to [3] it can also be expressed in the compact form $(\mathbf{A}\mathbf{M}^{-1}\mathbf{A}^T)^{-1}$ where \mathbf{M} is the mass matrix of the coupled human-device system using minimum set coordinate level representation, and \mathbf{A} is the Jacobian associated with the rendered directions. For a single rendered direction the general expression reduces to a scalar effective mass.

The effective mass can also be derived through a set of coordinate transformation. For this, as the first step the mass matrix has to be expressed with a different parametrization which directly include the m generalized velocities, \mathbf{u}_r , representing the rendered directions. The remaining $n - m$ generalized velocities, $\boldsymbol{\pi}_a$, are associated with some actual physical directions selected/chosen appropriately to easy the calculations, but otherwise they are arbitrary. Then the dynamic equation of motion can conveniently be decomposed as

$$\begin{bmatrix} \mathbf{W}_{rr} & \mathbf{W}_{ra} \\ \mathbf{W}_{ar} & \mathbf{W}_{aa} \end{bmatrix} \begin{bmatrix} \dot{\mathbf{u}}_r \\ \dot{\boldsymbol{\pi}}_a \end{bmatrix} + \begin{bmatrix} \mathbf{c}_r \\ \mathbf{c}_a \end{bmatrix} = \begin{bmatrix} \mathbf{f}_r \\ \mathbf{f}_a \end{bmatrix} \quad (1)$$

*On leave from HAS-BME Research Group on Dynamics of Machines and Vehicles, Műegyetem rkp. 5., 1111 Budapest, Hungary

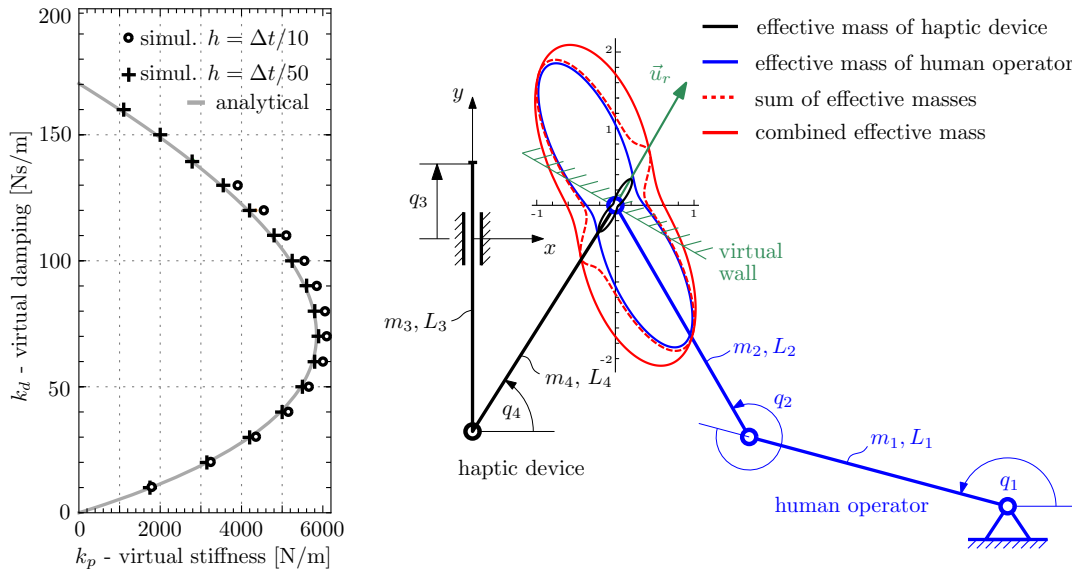


Figure 1: Calculated vs. simulated impedance ranges (left), Model with effective masses (right)

where \mathbf{W} is the mass matrix, \mathbf{c} is the array of Coriolis/centrifugal terms and \mathbf{f} stands for transformed actuator forces. Subscripts r and a refer to the rendered and the arbitrarily selected independent directions, respectively. In general, \mathbf{W} is a full matrix. However, by selecting a new set of coordinates as $\mathbf{u}_a = \boldsymbol{\pi}_a + \mathbf{B}\mathbf{u}_r$, where \mathbf{B} is an $(n - m) \times m$ yet unknown transformation matrix, the mass matrix can be decoupled. The resulting upper-left block will represent the effective inertia in the rendered directions. It can also be shown that the decoupling transformation needs $\mathbf{B} = \mathbf{W}_{aa}^{-1}\mathbf{W}_{ar}$, and the effective mass becomes

$$\mathbf{W}_{\text{eff}} = \mathbf{W}_{rr} - \mathbf{W}_{ra}\mathbf{W}_{aa}^{-1}\mathbf{W}_{ar} \quad (2)$$

The evaluation of this expression results in the same effective mass as $(\mathbf{A}\mathbf{M}^{-1}\mathbf{A}^T)^{-1}$ would give. An important difference, however, lies in the formulation of the problem. The new result presented here only requires the inversion of the mass matrix block that is associated with the admissible motions, and it makes possible the direct interpretation of the effects of the elements of the operational space mass matrix on the effective mass. For example, the second term in (2) has to be minimized in order to maximize the effective mass when that is desirable. This term may also vanish in certain cases.

To validate the use of the combined effective mass for characterizing the virtual contact dynamics a simulation study was conducted. A simple haptic device model and a two-link human model are considered with realistic kinematic and inertia parameters, and the impedance range of this multibody system was determined based on the basic haptic model in [2] and using the calculated effective mass of the combined system. This analytical prediction was verified by a series of experiments. With the selection of the rendered direction indicated by \vec{u}_r , the results are summarized in Fig. 1. This figure also demonstrates that the sum of the individual effective inertia parameters will not result in that of the combined system. The combined effective mass depends very much on the configuration of both the haptic device and the human operator, and also on the rendered direction. Therefore, the human model parameters currently available in the literature could only be used reliably, if they were obtained under very similar operating conditions as that of the specific parameter identification experiments. For a certain haptic device, this might partially be resolved by analysing the combined effective inertia parameters with age-, gender- and size-based multibody human arm models.

References

- [1] J.J. Gil, I. Diaz. Influence of Vibration Modes and Human Operator on the Stability of Haptic Rendering. IEEE Transactions on Robotics, Vol. 26, No. 1, pp. 160–165, 2010.
- [2] J.J. Gil, A. Avello, A. Rubio, J. Florez. Stability Analysis of a 1 DoF Haptic Interface Using the Routh-Hurwitz Criterion. IEEE Tran. on Control Syst. Tech., Vol. 12, No. 4, pp. 583–588, 2004.
- [3] O. Khatib. Inertial Properties in Robotic Manipulation: An Object-Level Framework. The International Journal of Robotics Research, Vol. 13, No. 1, pp. 19–36, 1995.